DOI: 10.6060/ivkkt.20246706.6996

УДК: 631.412

ОЦЕНКА УДЕЛЬНОЙ ПОВЕРХНОСТИ И ПОРИСТОСТИ ГРУНТОВ

Л.Д. Аснин, М.С. Самойлов, М.В. Першина, Ю.Г. Целищев, Н.Н. Слюсарь

Леонид Давыдович Аснин (ORCID 0000-0001-6309-6140)*, Михаил Сергеевич Самойлов (ORCID 0000-0002-6967-0542), Маргарита Владимировна Першина (ORCID 0000-0002-2576-3501), Наталья Николаевна Слюсарь (ORCID 0000-0003-0123-6907)

Пермский национальный исследовательский политехнический университет, Комсомольский пр., 29, Пермь, Россия, 614000
E-mail: asninld@mail.ru*, samojlov23@yandex.ru, mvpersh@yandex.ru, nnslyusar@gmail.com

Юрий Геннадьевич Целищев

Институт Технической химии УрО РАН, ул. Академика Королева, 3, Пермь, Россия, 614013
E-mail: yu-tsl@yandex.ru

Почвы и грунты имеют сложное строение из нескольких элементов различной морфологии и химического состава, сочетающих микро-, мезо- и макропористую структуру. Классические подходы, такие как методы Брунауэра-Эммета-Теллера (BET) или Барретта-Джойнера-Халенды (BJH), не могут обеспечить точную оценку морфологических характеристик твердых тел, также как и современные сложные численные методы, которые зависят от идеализированных моделей пор, что вряд ли отражает реальную морфологию рассматриваемых гетерогенных твердых тел. Настоящее исследование описывает способ преодолеть эту трудность, применяя комбинацию методов α_s-кривой и модифицированного метода Реми-Понселе. Предложенный подход позволил оценить объемы ультрамикропор, супермикропор и сумму мезо- и макропор, а также удельную поверхность твердого тела без ультрамикропор и твердого тела без всех микропор. Удельная площадь поверхности без учета ультрамикропор является более разумной оценкой величины поверхности, чем площадь поверхности по БЭТ, и все вместе эти характеристики обеспечивают детальное описание морфологии твердого тела. В качестве материалов исследования использовались образцы грунта, извлеченные с разной глубины и состоящие в основном из кварца, полевого шпата и глинистых минералов. Образцы имели различного рода поры, что связано с содержанием глинистой фракции и наличием почвенных агрегатов, а также относительно большую долю непористых частиц песка. Обсуждается связь морфологических свойств между профилем грунтов и минералогическим составом.

Ключевые слова: микропоры, мезопоры, удельная поверхность, уравнение Дубинина-Радушкевича, уравнение БЭТ, грунт

ASSESSMENT OF SPECIFIC SURFACE AREA AND POROSITY OF SUBSOILS

L.D. Asnin, M.S. Samoylov, M.V. Pershina, Yu.G. Tselishchev, N.N. Sliusar

Leonid D. Asnin (ORCID 0000-0001-6309-6140)*, Mikhail S. Samoylov (ORCID 0000-0002-6967-0542), Margarita V. Pershina (ORCID 0000-0002-2576-3501), Nataliya N. Sliusar (ORCID 0000-0003-0123-6907)

Perm National Research Polytechnic University, Komsomolsky pr., 29, Perm, 614990, Russia
E-mail: asninld@mail.ru*, samojlov23@yandex.ru, mvpersh@yandex.ru, nnslyusar@gmail.com

Yurii G. Tselishchev

Institute of Technical Chemistry of the Ural Branch of the RAS, Academician Korolev st., 3, Perm, 614013, Russia
E-mail: yu-tsl@yandex.ru

Soils and subsoils have a complex structure consisting of several elements with different morphology and chemical composition, combining micro-, meso-, and macroporous substructures. Classical approaches, such as Brunauer-Emmett-Teller (BET) or Barrett-Joyner-Halenda (BJH) methods, cannot provide an accurate assessment of morphological characteristics of such solids, nor can do modern sophisticated numerical methods which depend on idealized models of pores that hardly reflect a real morphology of heterogeneous solids in question. The present study describes a way to overcome this difficulty by applying a combination of the α_S-plot technique and a modified Remy-Poncelet method. The proposed approach allowed estimating the volumes of the untramicropores, supermicropores and the sum of meso- and macropores as well as the specific surface areas of the solid without ultramicropores and of the solid without all micropores. The former specific surface area is a more reasonable estimate of the area available for layer coverage than the BET specific surface area, and all together these characteristics provide a detail description of solid's morphology. Subsoil samples excavated from different depths were used as exemplary solids. They mostly consisted of quartz, feldspar, and clay minerals and had different sorts of pores associated with the clay fraction and soil aggregates as well as a relatively large fraction of non-porous sand particles. Relations of the morphological properties with subsoil profile and mineralogical composition are discussed.

Keywords: micropores, mesopores, specific surface area, Dubinin-Radushkevich equation, BET equation, subsoils

Для цитирования:
Аснин Л.Д., Самойлов М.С., Першина М.В., Целищев Ю.Г., Слюсарь Н.Н. Оценка удельной поверхности и пористости грунтов. *Изв. вузов. Химия и хим. технология*. 2024. Т. 67. Вып. 6. С. 55–64. DOI: 10.6060/ivkkt.20246706.6996.

For citation:
Asnin L.D., Samoylov M.S., Pershina M.V., Tselishchev Yu.G., Sliusar N.N. Assessment of specific surface area and porosity of subsoils. *ChemChemTech [Izv. Vyssh. Uchebn. Zaved. Khim. Khim. Tekhnol.]*. 2024. V. 67. N 6. P. 55–64. DOI: 10.6060/ivkkt.20246706.6996.

INTRODUCTION

Specific surface area and specific pore volume (porosity) are important characteristics of soils influencing their adsorption capacity and reactivity with respect to pollutans, filtration properties, and retention of moisture. Among several methods to measure specific surface area, the low-temperature nitrogen adsorption technique is especially popular [1-4], because there are precise and automated instruments that make measurements relatively easy, fast, and reproducible. On the other hand, the interpretation of experimental data still may pose essential difficulties. Unambiguous determination is possible only for non-porous and macroporous solids [1]. The characterization of pure microporous and pure mesoporous solids, although depends on assumptions regarding the shape of pores, can be made with fair certainty [2, 5]. Attempts were made to estimate morphological characteristics of micro/mesoporous materials based on the *t*- and α_S-methods [6, 7], on a combination of the Brunauer-Emmett-Teller (BET)-method and the *n*-nonane preadsorption technique [8], and on sophisticated numerical calculations of pore size distribution (PSD) using Monte-Carlo molecular simulations [9] or different modifications of the density functional theory [10, 11]. These listed works and many others, which cannot be cited for the sake of brevity, consider solids as a combination of pores of different size, without any flat surface. At the same time, many materials are composed of an essential nonporous fraction along with microporous, mesoporous, and macroporous parts. Subsoils are a typical example of such composite solids. They contain the non-porous sand fraction consisting of irregularly shaped microparticles of quartz, feldspar, calcite etc and the microporous clay fraction (unlike topsoil, subsoil does not contain organic matter). Agglomerates formed by microparticles give rise to mesopores in the crevices between contiguous microparticles and macropores in the cavities of these agglomerates. The resulting material hardly fits in any of the idealized pore models (slit-shaped, cylindrical, spherical) used to calculate PSD, and even more sophisticated hybrid models [12, 13] do not describe it adequately as assume the solid to be chemically homogeneous that is not the case with subsoils.

Because the applicability of advanced techniques to characterize heterogeneous pore structures is a topic of debates, on the one hand, and these techniques

frighten off researchers by their mathematical complexity, on the other hand, simple approaches are still of interest and relevance. In the present communication, proceeding from earlier ideas by Dubinin and Kadlec [14] and Remy and Poncelet [15] an approach was developed for accurate measurement of a set of morphological characteristics relating to specific surface area and pore structure, describing different fractions of the pores. The application of the α_s-plot method to such heterogeneous and polydisperse materials as (sub)soils is also discussed. This approach was applied to display subtle changes in the morphological structure of subsoils accompanying variations in their mineralogical composition along the subsoil profile.

THEORETICAL

Adsorption on non-porous and macroporous solids

Adsorption of gases on such solids (pore size > 50 nm) proceeds in a layered fashion. Gas molecules being adsorbed on the solid surface form the first layer and may serve as adsorption sites for other gas molecules. Thus on the top of the first layer the second adsorbed layer forms and so on. The most popular model describing the multilayer adsorption is the BET model [2]. The respective adsorption isotherm equation relates the adsorbed amount expressed here as the volume of liquid adsorbate, V, to equilibrium relative pressure, $x = p/p_0$ (p being the adsorptive pressure and p_0 the saturated adsorptive vapor pressure), as follows

$$V = \frac{V_m C x}{(1-x)[1+(C-1)x]} \quad (1)$$

where V_m is the monolayer volume and C the constant relating to the energy of adsorption of the first monolayer. The volume of monolayer relates to the specific surface area as

$$S = V_m \rho N_A \sigma \quad (2)$$

with N_A being the Avogadro number, ρ and σ being the molar density and cross-sectional area of a probe adsorbate, usually nitrogen.

Adsorption on microporous solids

The size of the micropores is below 2 nm. In such small pores, adsorption forces of the pore walls overlap that produces enchanted adsorption energy leading to the filling of the whole pore at very low pressures. Consequently, the pore volume rather than the area of the pore walls is a representative morphological characteristic of the micropores.

The theory of volume filling of micropores [2] suggests the Dubinin-Radushkevich (DR) equation to relate the adsorbate volume in micropores, V_{mi}, to the relative pressure:

$$V_{mi} = W_0 \exp[(-A/E)^2] \quad (3)$$

where W_0 is the volume of micropores, E the characteristic adsorption energy and A the differential molar work of adsorption, $A = RT\ln(p_0/p)$, being R the gas constant and T the absolute temperature.

Adsorption on heterogeneously porous solids

In general case, such solids contain all sorts of pores, micropores filled by the volume filling mechanism, mesopores (2-50 nm) where the surface coverage mechanism takes place at low pressures and capillary condensation can happen at $x > 0.4$, and macropores and flat surface where adsorption proceeds by the surface coverage mechanism. Dubinin and Kadlec [14] and later Schneider [16] proposed to divide the total adsorbed amount into the parts adsorbed by the micropores, V_{mi}, and by the larger pores, V_{ext}: $V = V_{mi} + V_{ext}$.

In the Dubinin and Kadlec method, the filling of the micropores was supposed to obey to the DR equation and a model for the adsorption in the larger pores was not specified, while in the Schneider method the micropore contribution, $V_{mi,0}$, was assumed to be constant and V_{ext} was a BET-function of the relative pressure.

The next logical step was made by Remy and Poncelet [15] who combined the DR and BET equations so that

$$V = W_0 \exp\left[-\left(\frac{RT \ln\left(\frac{1}{x}\right)}{E}\right)^2\right] + \frac{V_m C x}{(1-x)[1+(C-1)x]} \quad (4)$$

The approximation of experimental data by Eq. (4) yields four fitting parameters: W_0, E, C, and V_m. From the latter, the external specific surface area is computed by Eq. (2). This approach was discussed in few studies [17 and Refs. therein]. Buttersack et al. [17] mentioned the problem of interdependence of the fitting parameters resulting in some uncertainty in the morphological characteristics. More reliable estimates can be obtained if the procedures of determination of W_0, E and C, V_m are separated and performed under conditions most favorable for accurate measurement of the respective structural characteristics. To this end, low temperature nitrogen adsorption measurements at two relative pressure ranges were performed. To evaluate W_0 and E, the measurements must be made at very low x values, not far from the point of complete filling of the micropores. As the relative pressure upper limit is low, the x step must be very small in order to obtain sufficient number of data points for accurate approximation. Knowing W_0 and E, one can derive C and V_m parameters from adsorption isotherm data measured over a wide x range, up to the onset of capillary condensation, using Eq. (4). The pressure step in this experiment can be relatively large to allow fast measurements.

EXPERIMENTAL

Samples

Samples were excavated from two drilled boreholes, designated 1 and 2, respectively, located on a distance of 100 m from each other in a wasteland on the north edge of the city of Perm, Russia (57°58′ N, 56°12′ E). The study area consisted of Upper Quaternary alluvial deposits of 8-9 m thickness overlying Lower Permian sediments mostly represented by argillite (Fig. 1). The samples were collected in the form of cores with a diameter of 0.1 m and height of 1 m from successive depths in the interval 0-10 m. The top soil layer of 0.1 m thickness was removed. The samples were air-dried at room temperature for a week, gently ground to pass through a 3-mm sieve and sieved through a set of wire mesh sieves (3.0, 2.0, 1.0, 0.5, 0.25, and 0.1 mm). The fraction 0.1-0.25 mm was taken for further study.

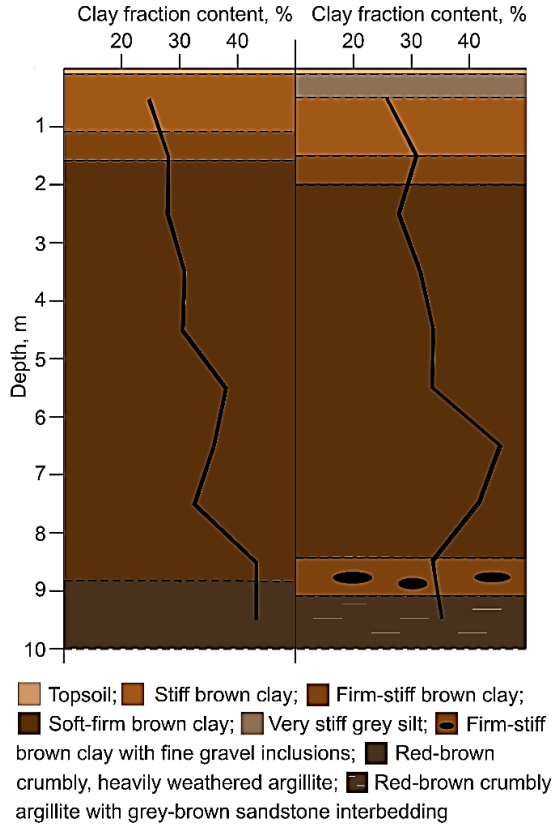

Fig. 1. Lithology columns and clay content (solid lines) for borehole 1 (left) and borehole 2 (right)

Рис. 1. Литологические колонки и содержание глинистой фракции (сплошные линии) для скв. 1 (слева) и скв. 2 (справа)

Quantitative mineralogical analysis

The X-ray diffraction (XRD) patterns were recorded on a D2 PHASER diffractometer (Bruker, Germany) equipped with a linear LynxEye detector, with Ni-filtered Cu-Kα radiation (λ = 1.5406 Å) with the X-ray tube operated at 30 kV and 10 mA. The beam was collimated using a 0.2 mm divergence slit and two Soller slits, both of 2.5°. The overall mineralogical composition was determined by the random powder method, with samples rotated over the angular range of 5 to 70° 2θ using a step interval of 0.02° and a counting time per step of 1 s. The computation of the relative contents of the mineral phases was performed using the Diffrac.Topas 4.2 (Bruker, Germany) software by means of the etalon-free Rietveld method [18]. The composition of the clay fraction (< 5 μm, obtained by sedimentation) was determined by the oriented slides method [19], with the diagrams recorded from 4.5 to 35° of 2θ using the same step interval and counting time as above. The XRD patterns of the raw clay fraction, the clay fraction saturated with ethylene glycol vapors or heated to 380 and 550 °C for 1 h were obtained to identify clay minerals [19]. The quantification was carried out by reflection areas applying the Diffrac.Eva (Bruker, Germany) software.

Low-temperature nitrogen adsorption

The nitrogen adsorption isotherms were measured using an ASAP 2020MP (Micromeritics, USA) analyzer at -196 °C. The samples, 0.5-0.7 g, preliminary air-dried at 70 °C for 12 h were additionally outgassed in vacuum at the degassing port of the analyzer at 90 °C for 3.5 h. For the assessment of the specific surface area by BET method and the overall porosity by Barrett-Joyner-Halenda method, the measurements were carried out over a range of x from ca. 0.005 to 1 with a step of 0.005-0.05. The BET specific surface area, S_{BET}, was calculated from linearized BET plots applying the Rouquerol rules [20] to locate the linear range of the BET plots. Usually, it was within the relative pressure range of 0.03-0.20. The overall pore volume and the total surface area by BJH method were derived from the desorption branch of adsorption isotherms using the ASAP 2020 Plus software from Micromeritics.

For the assessment of microporosity by a modified Remy-Poncelet method, the adsorption data were obtained at a low pressure range, x increasing from 0 to 0.005 with a step of 10^{-6}–$5 \cdot 10^{-4}$. As pressure was very low, obviously within the linear range of the (local) nitrogen adsorption isotherm on the external surface, Eq. (4) was simplified replacing the BET term with a linear term so that

$$V = W_0 \, exp\left[-\left(\frac{RT \, ln\left(\frac{1}{x}\right)}{E}\right)^2\right] + Kx \qquad (5)$$

being K an adjustable parameter. The number of adjustable parameters was decreased to 3, increasing the

robustness of the fitting procedure. Eq. (5) approximated the experimental data perfectly, the determination coefficient, r^2, never being less than 0.99.

α_s-plots

The α_s-plot method, an analogue of the *t*-plot method, is a way of analyzing solid morphology by comparing nitrogen adsorption isotherms on a given solid to that measured on a non-porous reference solid [2]. The quantity α_s is the ratio of the adsorbed amount to that adsorbed at a specific relative pressure *x*. In the given study, $x = 0.4$ in accordance with the recommendation by Gregg and Sing [2]; thus $\alpha_s = V/V_{0.4}$, where $V_{0.4} = V(x = 0.4)$. The α_s-plot is a graph of the amount of nitrogen adsorbed on a test sample against α_s for the adsorption of nitrogen on a reference solid taken at the same relative pressure. The slope of an α_s-plot is proportional to the specific surface area, and the latter can be derived from it using the following expression:

$$S = S_{ref}\frac{Slope}{(V_{0.4})_{ref}} \quad (6)$$

where the subscript 'ref' refers to the reference solid. The solid of the same chemical nature was used as a reference material in study [2]. In the present work, there was used non-porous spherical silica with particle size 3 μm supplied by Glantreo (Ireland) as the reference solid (S_{ref} = 1.53 m^2/g).

RESULTS AND DISCUSSION

Nitrogen adsorption isotherms, x = 0 – 0.005

A typical adsorption isotherm in the low pressure area is shown in Fig. 2. Neither the DR equation nor more sophisticated Dubinin-Astakhov equation [2] (not reported data) could approximate the experimental data well, while Eq. (5) did it perfectly. Table 1 summarizes the best-fit parameters obtained in these calculations. The non-microporous contribution (term *Kx* in Eq. (5)) to the overall adsorption at $x = 0.005$ amounted to noticeable 10-14%. The characteristic adsorption energy was ca. 6 kJ/mole. This is a relatively low value as *E* typically varies within 15-40 kJ/mole for clay minerals and other porous aluminosilicate materials [21-24], although figures less than 6 kJ/mol were occasionally found [17, 25, 26]. The *E* value is known to be inversely proportional to an average linear dimension of the micropores [27]; however, there is no a quantitative relation that would allow converting *E* to a representative pore dimension like one obtained for carbonaceous adsorbents [27]. According to the literature data [17, 21-26] *E* depends not only on the pore size but also on the solid's chemical nature. At the same time, the examined literature suggests that it is unlikely that a solid characterized by *E* values shown in Table 1 would have micropores with an average width smaller than 1 nm.

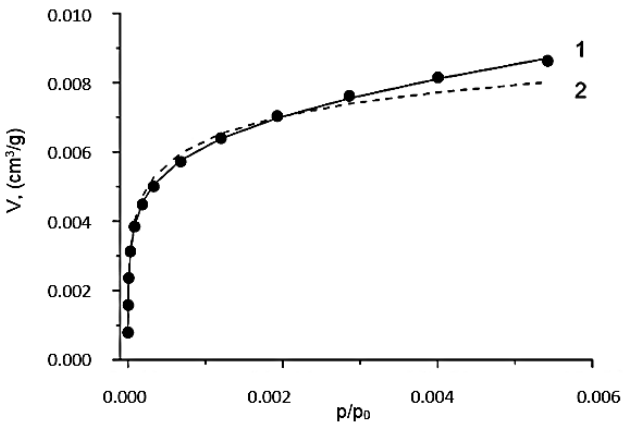

Fig. 2. A nitrogen adsorption isotherm measured over the micropore filling range. Experimental data, symbols: 1 – approximation by the extended DR equation (Eq. (7)), solid line; 2 – approximation by the DR equation, dashed line

Рис. 2. Изотерма адсорбции азота, измеренная в диапазоне заполнения микропор. Экспериментальные данные, обозначения: 1 – аппроксимация расширенным уравнением ДР (уравнение (7)), сплошная линия; 2 – аппроксимация уравнением ДР, пунктирная линия

Table 1

Best-fit coefficients of the extended Dubinin-Radushkevich equation

***Таблица 1.* Коэффициенты наилучшего соответствия расширенного уравнения Дубинина-Радушкевича**

	Borehole 1			Borehole 2		
Depth, m	*K* (cm^3/g)	W_0 (cm^3/g)	*E* (J/mole)	*K* (cm^3/g)	W_0 (cm^3/g)	*E* (J/mole)
0 – 1	141.5	0.0108	6407	111.1	0.0080	6251
1 – 2	168.9	0.0109	6423	147.7	0.0102	6286
2 – 3	157.1	0.0099	6221	113.6	0.0093	6285
3 – 4	120.4	0.0110	6389	125.9	0.0096	6334
4 – 5	167.5	0.0100	6376	149.1	0.0106	6351
5 – 6	140.3	0.0102	6477	165.0	0.0134	6330
6 – 7	110.9	0.0087	6290	177.3	0.0136	6434
7 – 8	140.7	0.0099	6370	202.6	0.0123	6370
8 – 9	110.1	0.0090	6336	93.7	0.0075	6356
9 – 10	74.5	0.0090	6293	79.7	0.0075	6168

Nitrogen adsorption isotherms, x = 0.005 –1

Adsorption isotherms of all investigated samples demonstrate a hysteresis loop of H3 type, revealing a fraction of mesopores. Such a type of hysteresis loop was characteristic to aggregates of plate-like particles usually found in certain clays [5, 28]. Indeed, the XRD analysis found 25 to 45 percent of clay minerals in the samples (Fig. 1). The prevailing clay mineral in both boreholes is smectite. Its content increased with the sampling depth, while that of illite decreased. α_s-plots (Fig. 3) exposes the presence of a small fraction of micropores. The plot can be divided in two regions characterized by different slopes. Similar α_s-plots have

been reported for pillared clays [29] and some aluminosilicate minerals [30]. The low pressure part of the plot corresponds to the surface left after filling the micropores, their volume believed to be given by the intercept of the linear region extrapolated to the ordinate [2]. These pores are filled at relative pressure below 0.006 (value at which α_s-plots start) and therefore are most probably ultramicropores or small supermicropores with size about or slightly larger than 0.7 nm. The break in the α_s-plot is apparently explained by pores being closed by the adsorbed layer. Converting α_s values to the thickness of the adsorbed layer by Eq. (7), one can conclude that given the pores are slit-shaped their width corresponding to the break point is 1.0–1.4 nm (Table 2).

$$\frac{t}{\text{nm}} = 0.354 \frac{V_{0.4}}{V_m} \alpha_s \qquad (7)$$

The slope of the second part of the α_s-plot gives the remaining specific surface area of the wider pores and the non-porous sand particles. The mesopores should manifest themselves by an upward deviation of the α_s-plot from a straight line at the high pressure region, owing to capillary condensation. No such effect was observed in any of the studied samples. On the other hand, the presence of mesopores is revealed by the hysteresis loop in adsorption/desorption isotherms. This is not surprising. Sing and Williams [28] noticed that the H3 type hysteresis loops were typical for materials with no well-defined mesopore volume. This does not contradict to Broeckhoff and de Boer [31] hypothesizing that the absence of the capillary condensation effect on the adsorption branch was possible for slit- or wedge-shaped pores which were expected for aggregates of clay and sand. Indeed, poorly developed mesoporosity can consist of slit-shaped pores, and the lack of the capillary condensation effect can be obscured in comparison plots because of either factor.

The intercept of the second linear fit with the Y-axis, by its physical meaning, must be the volume of the pores occupied by adsorbed nitrogen up to the point from which this line starts. Galarneau et al. did not agree with such an interpretation, and advocated based on the experimental data obtained with hierarchical zeolites the use of the ordinate of the break point as an estimate of the overall micropore volume [6, 32]. The present data do not support such an attribution for the studied samples. The break point corresponds to relative pressure 0.4-0.7. At these values were not only the micropores but also a part of the mesopores is filled according to the hysteresis loops observed. Thus, V_b cannot be ascribed a definite physical meaning like it was possible for the hierarchical zeolites. It is an intermediate characteristic, which is larger than the volume of micropores but smaller than the volume of micropores plus mesopores. Quantitatively, it accounts for 40-70% of the total pore volume, V_{tot}. The latter quantity was derived from the amount adsorbed at a relative pressure of 0.95 following IUPAC recommendations [5]. Although the BJH method is not recommended for the H3 type isotherms [28], the cumulative BJH pore volume, V_{BJH}, was computed as one more estimation of the total pore volume for the sake of comparison.

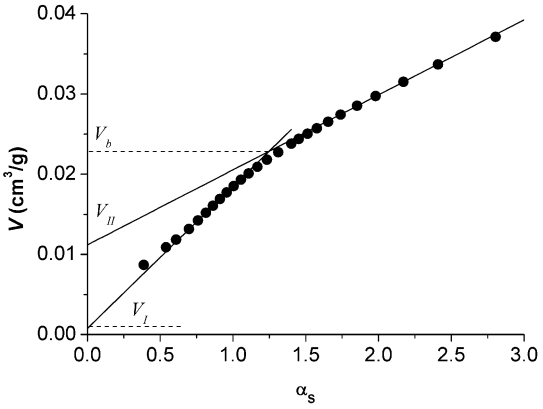

Fig. 3. An α_S-plot for the same sample as in Fig. 2 plotted over the relative pressure range 0.006-0.955. Note V_I, the intercept of the first (low pressure) linear fit; V_{II}, the intercept of the second (high pressure) linear fit; and V_b, the ordinate of the intersection point of the first and second linear fits (break point)

Рис. 3. α_S–график для того же образца, что и на рис. 2, в диапазоне относительных давлений 0,006-0,955. Примечание: V_I – точка пересечения первой линейной аппроксимации (низкое давление); V_{II} – точка пересечения второй (высокого давления) линейной посадки; и V_b – ордината точки пересечения первой и второй линейных подгонок (точка разрыва)

Table 2

Specific surface areas and C coefficients obtained by different methods [a, b]

***Таблица 2*. Удельная поверхность и коэффициенты C, полученные разными методами [a, b]**

	BET equation		BJH method	α_S-plot method			Remy-Poncelet equation (Eq. 6)	
Depth, m	C (–)	S_{BET} (m²/g)	S_{BJH} (m²/g)	S_I (m²/g)	S_{II} (m²/g)	$2t_b$ [b] (nm)	C (–)	$S_{V\text{-}DR}$ (m²/g)
	Borehole 1							
0 – 1	182	36.2	29.4	32.5	15.1	1.4	6.4	15.1
1 – 2	172	37.7	30.4	35.0	16.9	1.3	7.2	16.5

Продолжение таблицы

2 – 3	154	35.0	29.7	33.6	17.7	1.3	11.0	16.7
3 – 4	186	36.2	28.8	31.7	15.7	1.3	9.8	15.4
4 – 5	164	35.1	30.1	33.1	18.7	1.3	6.6	15.4
5 – 6	188	33.3	27.7	29.2	19.0	1.2	5.3	13.5
6 – 7	176	30.3	27.3	28.2	20.5	1.1	8.8	13.5
7 – 8	172	33.6	28.9	31.1	19.5	1.3	6.1	14.4
8 – 9	176	29.8	28.3	27.5	21.2	1.0	8.2	13.1
9 – 10	176	28.2	26.7	26.6	19.3	1.1	6.0	12.4
Borehole 2								
0 – 1	183	28.0	25.0	26.6	14.9	1.4	10.6	13.3
1 – 2	199	35.1	29.1	33.0	15.8	1.4	11.3	16.3
2 – 3	184	31.0	25.0	27.6	15.1	1.3	9.7	13.8
3 – 4	186	32.0	26.2	29.1	15.3	1.3	6.4	13.7
4 – 5	180	35.7	29.8	32.5	17.9	1.3	6.6	15.1
5 – 6	194	44.3	35.3	38.2	16.1	1.3	9.8	18.5
6 – 7	219	44.5	36.9	37.9	21.3	1.3	7.2	17.6
7 – 8	193	42.2	37.2	39.6	27.4	1.3	6.9	18.5
8 – 9	200	23.6	22.2	21.1	16.7	1.0	4.7	9.7
9 – 10	210	26.8	24.9	23.0	17.3	1.1	9.1	11.1

Notes: [a] data are rounded to the first uncertain digit;
[b] t_b is the statistical thickness of the adsorbed layer corresponding to the break point of the α_S-plot
Примечания: [a] данные округляются до первой неопределенной цифры; [b] t_b — статистическая толщина адсорбированного слоя, соответствующая точке излома α_S-графика

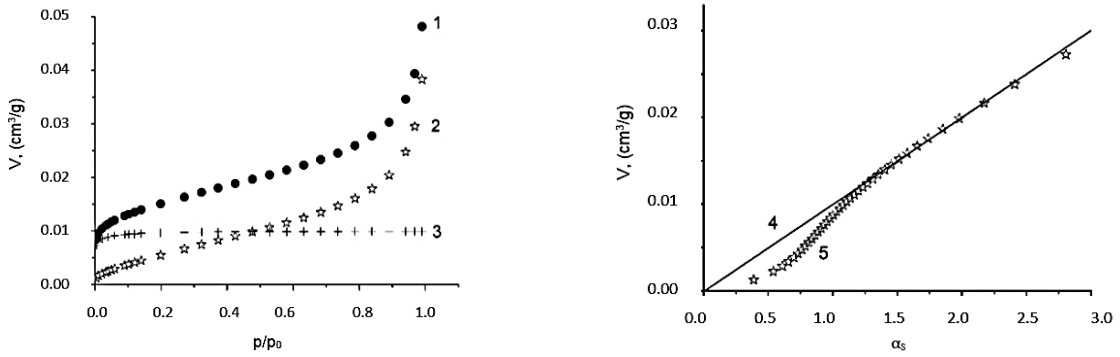

Fig. 4. (A) A corrected nitrogen adsorption isotherm (2, star symbols) calculated from an original isotherm (1, closed circles) by subtracting the amount adsorbed in the micropores evaluated by the DR equation (3, cross symbols). (B) Tangent line (4) to the α_s-plot corresponding to the corrected adsorption isotherm (5). The same sample as in Fig. 2

Рис. 4. (А) Скорректированная изотерма адсорбции азота (2, звездочки), рассчитанная из исходной изотермы (1, темные кружки) путем вычитания количества, адсорбированного в микропорах, оцененного по уравнению ДР (3, крестики). (В) Касательная (4) к α_s-графику для скорректированной изотермы адсорбции (5). Тот же образец, что и на рис. 2

Using Eq. (4) with the W_0 and E values found in Section 4.1, one can subtract the effect of microporosity from the total adsorbed amount to study the adsorption by meso- and macroporous elements and by non-porous particles. The resulting curve is a Type II isotherm (Fig. 4A). Their characteristic parameters, specific surface area, $S_{V\text{-}DR}$, and coefficient C, are given in Table 2. As seen, the C constant values are smaller than those for original isotherms by an order of magnitude. Relatively high original C values are accounted for by adsorption of nitrogen in micropores, which are mostly associated with the clay fraction, and do not represent the chemical nature of the "non-microporous" surface composed of sand particles and the external surface of clay aggregates. The α_s-plots corresponding to the corrected isotherms show a tendency to the origin, indicating the removal of the micropore contribution (Fig. 4B).

Morphological characteristics

Different estimates of the specific surface area are compared in Table 2. The BET method is seen to deliver the highest estimate of S. The specific surface area values obtained by the BJH method and derived from the α_S-plot (the first value, S_I) are comparable and

both were less than S_{BET} by 1-9 m^2/g (S_I is somewhat larger than S_{BJH}, except in the last two sections). Perhaps, this increment relates somehow to the micropores (S_{BJH} was computed for pores larger than 1.7 nm), but whether this value is the area of the micropore walls remained questionable. Assuming slit-shaped pores, this increment gives a micropore size of 2-9 nm based on W_o as the micropore volume. Obviously, this is too large an estimate suggesting that the difference between S_{BET} and S_I (S_{BJH}) is due to both the pores accommodating only two monomolecular layers and somewhat larger pores but within the domain of micropores.

The S_{II} and $S_{V\text{-}DR}$ values are comparable at sampling depths less than 6 m, and $S_{V\text{-}DR} < S_{II}$ at deeper horizons, where both the clay content and the smectite percentage are larger. Those quantities estimate the surface remaining unoccupied after the micropores or a larger fraction of the latter are filled. The areas described by these quantities do not coincide, and the discrepancy consists in a fraction of large micropores (1.0-1.4 to 2 nm) and/or narrow mesopores associated with the clay matter.

Table 3

Estimates of the pore volume (cm^3/g) obtained by different methods [a,b]

Таблица 3. **Оценки объема пор ($см^3/г$), полученные разными методами [а,б]**

Depth (m)	V_{tot}	V_{BJH}	V_b	V_I	V_{II}
	Borehole 1				
0 – 1	0.0348	0.0393	0.0241	0.0017	0.0136
1 – 2	0.0370	0.0423	0.0245	0.0013	0.0132
2 – 3	0.0359	0.0437	0.0228	0.0008	0.0112
3 – 4	0.0344	0.0404	0.0227	0.0020	0.0124
4 – 5	0.0364	0.0448	0.0221	0.0010	0.0101
5 – 6	0.0350	0.0451	0.0192	0.0019	0.0078
6 – 7	0.0350	0.0465	0.0173	0.0011	0.0053
7 – 8	0.0364	0.0463	0.0207	0.0012	0.0083
8 – 9	0.0350	0.0480	0.0159	0.0011	0.0043
9 – 10	0.0327	0.0439	0.0159	0.0009	0.0048
	Borehole 2				
0 – 1	0.0302	0.0355	0.0202	0.0008	0.0093
1 – 2	0.0350	0.0393	0.0236	0.0011	0.0129
2 – 3	0.0312	0.0365	0.0200	0.0017	0.0099
3 – 4	0.0325	0.0376	0.0210	0.0015	0.0105
4 – 5	0.0366	0.0475	0.0230	0.0015	0.0111
5 – 6	0.0402	0.0444	0.0286	0.0028	0.0176
6 – 7	0.0441	0.0547	0.0281	0.0030	0.0139
7 – 8	0.0484	0.0638	0.0274	0.0014	0.0094
8 – 9	0.0272	0.0441	0.0114	0.0012	0.0036
9 – 10	0.0298	0.0428	0.0143	0.0017	0.0049

Notes: [a] data are rounded to the first uncertain digit;
[b] Estimates of the micropore volume W_0 are given in Table 1
Примечания: [а] данные округляются до первой неопределенной цифры; [б] оценки объема микропор W_0 приведены в табл. 1

The cumulative pore volume by the BJH method exceeds the V_{tot} value (Table 3). The discrepancy is the larger, the higher the clay percentage in the samples. Of the two characteristics of the microporosity, V_I and W_0, the latter is 4-12 times larger than the former. V_I corresponds to ultramicropores and W_0 corresponds to overall micropores including supermicropores and, probably, narrow mesopores, which are not wider than 3.2 nm, the upper size limit suggested by Dubinin for the pores filled by the volume filling mechanism [33].

The volume V_{II} was related above to the sum of ultramicropores and supermicropores. It was of the same order of magnitude as W_0 but somewhat larger for the upper half of the boreholes and smaller for the lower half, again showing dependence on the mineralogical composition of samples. Taking into account that the attribution of V_{II} to the pores narrower than 1.0-1.4 nm was based on speculative assumptions, W_0 was considered as a more reliable estimate of the total micropore volume. Thus, the present data allowed ascribing 2 to 7% of the porous space to the ultramicropores (< 0.7 nm), 22 to 29% to the supermicropores and narrow mesopores (0.7-3.2 nm), the rest comprising the meso- and macropores.

Morphological characteristics of subsoil as a function of sampling depth

Even if the two studied boreholes belonged to the same geological formation, there is a difference in their soil profiles (Fig. 1) reflected in the profiles of mineralogical content. On the microstructural level, there are differences in the dependences of morphological characteristics on the sampling depth. While in borehole 1 S_I slowly and fluctuatively decreases with depth, the fluctuations resembling those in the clay content profiles, thus suggesting their nonrandom nature, S_I in borehole 2 has a maximum between 5 and 8 m. A similar maximum is seen in the clay content profiles and the profiles of other morphological characteristics ($S_{V\text{-}DR}$, W_0, V_{tot}). The fact that $S_{V\text{-}DR}$ (should be free from the effect of micropores) and W_0 change correlatively suggests that both quantities depend on another parameter, most likely the clay content. Indeed, the clay fraction is composed of microparticles (< 5 μm), whose specific external specific surface area is large due to their small size. This specific surface area is a part of the $S_{V\text{-}DR}$ value that results in a correlation between this characteristic and the clay percentage and, ultimately, the sampling depth. Of course, the variation of the total clay content over a borehole alone cannot explain the effect of the sampling depth on specific surface area and pore volume. Morphological characteristics also depend on types and relative contents of clay minerals,

composition of the sand fraction, chemical surface composition that defined the structure of soil aggregates etc. A detail investigation of the influence of these factors on the morphological characteristics is out of scope of this paper and could be discussed elsewhere.

CONCLUSIONS

A combination of the BET and DR analysis, the α_s-plot method and Remy-Poncelet method delivers an extended understanding of the morphological structure of polydisprese and heterogeneous solids. It allows us to characterize different fractions of pores. In the present study, using subsoil samples, the fractions of ultramicropores, supermicropores and larger pores were evaluated with a fair certainty proven by a reasonable agreement of the pore volumes found by different approaches. To obtain the total volume of micropores, the extended DR equation must be used, as the contribution of non-porous particles is noticeable even at the low pressure range where the DR analysis is applied. The BET analysis yields a somewhat overestimated value of the specific surface area available for layer filling (including the layer filling of the walls of supermicropores) due to the effect of the unltramicropores; however, the α_s-plot method gives a reliable estimation of this characteristic. The specific surface area of the solid minus its microporous part can be obtained by means of the Remy-Poncelet method.

Subsoil morphological characteristics are significantly accounted for by the total clay content. The studied subsoils containing 25 to 45% of clay of smectite (predominantly)-illite type have relatively low total pore volume (0.03-0.05 cm^3/g) composed by roughly 70% of the meso- and macropores, by 22-29% of the supermicropores, with the remaining minor fraction of the ultramicropores. The specific surface area of the samples varies between 20 and 40 m^2/g.

ACKNOWLEDGEMENT

The authors are thankful to Elena Tomilina (Perm State University) for the XRD measurements.

The authors declare the absence a conflict of interest warranting disclosure in this article.

Авторы благодарны Елене Томилиной (Пермский государственный национальный исследовательский университет) за рентгеноструктурные измерения.

Авторы заявляют об отсутствии конфликта интересов, требующего раскрытия в данной статье.

REFERENCES
ЛИТЕРАТУРА

1. **Heister K.** The measurement of the specific surface area of soils by gas and polar liquid adsorption methods—Limitations and potentials. *Geoderma*. 2014. V. 216. P. 75–87. DOI: 10.1016/j.geoderma.2013.10.015.
2. **Rouquerol F., Rouquerol J., Sing K.S.W., Llewellyn P., Maurin G.** Adsorption by Powders and Porous Solids: Principles, Methodology and Applications. San Diego, CA: Academic Press. 2013. 646 p.
3. **Фарберова Е.А., Максимов А.С., Ширкунов А.С., Рябов В.Г., Тиньгаева Е.А., Стрелков В.А.** Исследование возможности переработки нефтяного кокса с повышенным содержанием летучих веществ в углеродные сорбенты. *Изв. вузов. Химия и хим. технология.* 2021. Т. 64. Вып. 4. С. 92-99. DOI: 10.6060/ivkkt. 20216404.6331.
Farberova E.A., Maximov A.S., Shirkunov A.S., Ryabov V.G., Tingaeva E.A., Strelkov V.A. Research of possibility of processing petroleum coke with increased volatile substances into activated carbons. *ChemChemTech [Izv. Vyssh. Uchebn. Zaved. Khim. Khim. Tekhnol.].* 2021. V. 64. N 4. P. 92-99. DOI: 10.6060/ivkkt. 20216404.6331.
4. **Опра Д.П., Синебрюхов С.Л., Неумоин А.И., Подгорбунский А.Б., Гнеденков С.В.** Мезопористые нанотрубчатые материалы на основе $Na_2Ti_3O_7$ с иерархической архитектурой: синтез и свойства. *Изв. вузов. Химия и хим. технология.* 2022. Т. 65. Вып. 12. С. 37-43. DOI: 10.6060/ivkkt.20226512.6552.
Opra D.P., Sinebryukhov S.L., Neumoin A.I., Podgorbunsky A.B., Gnedenkov S.V. Mesoporous $Na_2Ti_3O_7$ nanotube-constructed materials with hierarchical architecture: synthesis and properties. *ChemChemTech [Izv. Vyssh. Uchebn. Zaved. Khim. Khim. Tekhnol.]*. 2022. V. 65. N 12. P. 37-43. DOI: 10.6060/ivkkt.20226512.6552.
5. **Thommes M., Kaneko K., Neimark A.V., Olivier J.P., Rodriguez-Reinoso F., Rouquerol J., Sing K.S.W.** Physisorption of gases, with special reference to the evaluation of surface area and pore size distribution (IUPAC Technical Report). *Pure Appl. Chem.* 2015. V. 87. N 9-10. P. 1051-1069. DOI: 10.1515/pac-2014-1117.
6. **Galarneau A., Mehlhorn D., Guenneau F., Coasne B., Villemot F., Minoux D., Aquino C., Dath J.-P.** Specific Surface Area Determination for Microporous/ Mesoporous Materials: The Case of Mesoporous FAU-Y Zeolites. *Langmuir*. 2018. V. 34. N 47. P. 14134-14142. DOI: 10.1021/acs.langmuir.8b02144.
7. **Prokešová-Fojtíková P., Mintova S., Čejka J., Žilková N., Zukal A.** Porosity of micro/mesoporous composites. *Micropor. Mesopor. Mater.* 2006. V. 92. P. 154-160. DOI: 10.1016/j.micromeso.2005.12.017.
8. **Batonneau-Gener I., Sachse A.** Determination of the Exact Microporous Volume and BET Surface Area in Hierarchical ZSM-5. *J. Phys. Chem.* 2019. V. 123. N 7. P. 4235-4242. DOI: 10.1021/acs.jpcc.8b11524.
9. **Parashar S., Ravikovitch P.I., Neimark A.V.** Molecular Modeling and Adsorption Characterization of Micro-Mesoporous Kerogen Nanostructures. *Energy Fuels.* 2022. V. 36. N 21. P. 13037-13049. DOI: 10.1021/acs.energyfuels.2c02876.
10. **Gun'ko V.** Composite materials: Textural characteristics. *Appl. Surf. Sci.* 2014. V. 307. P. 444-454. DOI: 10.1016/j.apsusc.2014.04.055.

11. **Neimark A.V., Lin Y., Ravikovitch P.I., Thommes M.** Quenched solid density functional theory and pore size analysis of micro-mesoporous carbons. *Carbon*. 2009. V. 47. N 7. P. 1617-1628. DOI: 10.1016/j.carbon.2009.01.050.
12. **Gor G.Y., Thommes M., Cychosz K., Neimark A.V.** Quenched solid density functional theory method for characterization of mesoporous carbons by nitrogen adsorption. *Carbon*. 2012. V. 50. N 4. P. 1583-1590. DOI: 10.1016/j.carbon.2011.11.037.
13. **Landers J., Gor G.Y., Neimark A.V.** Density functional theory methods for characterization of porous materials. *Colloid. Surf. A: Physicochem. and Eng. Asp*. 2013. V. 437. P. 3-32. DOI: 10.1016/j.colsurfa.2013.01.007.
14. **Dubinin M.M., Kadlec O.** New ways in determination of the parameters of porous structure of microporous carbonaceous adsorbents. *Carbon*. 1975. V. 13. N 4. P. 263-265. DOI: doi.org/10.1016/0008-6223(75)90026-3.
15. **Remy M.J., Poncelet G.** A New Approach to the Determination of the External Surface and Micropore Volume of Zeolites from the Nitrogen Adsorption Isotherm at 77 K. *J. Phys. Chem.* 1995. V. 99. N 2. P. 773-779. DOI: 10.1021/j100002a047.
16. **Schneider P., Hudec P., Solcova O.** Pore-volume and surface area in microporous–mesoporous solids. *Micropor. Mesopor. Mater*. 2008. V. 115. N 3. P. 491-496. DOI: 10.1016/j.micromeso.2008.02.024.
17. **Buttersack Ch., Mollmer J., Hofmann J., Glaser R.** Determination of micropore volume and external surface of zeolites. *Micropor. Mesopor. Mater*. 2016. V. 236. P. 63-70. DOI: 10.1016/j.micromeso.2016.08.018.
18. **Gualtieri A.F., Gatta G.D., Arletti R., Artioli G., Ballirano P., Cruciani G., Guagliardi A., Malferrari D., Masciocchi N., Scardi P.** Quantitative phase analysis using the Rietveld method: towards a procedure for checking the reliability and quality of the results. *Mineral. Crystallogr.* 2019. V. 88. N 2. P. 147-151. DOI: 10.2451/2019PM870.
19. **Bergaya F., Lagaly G.** Handbook of Clay Science. Amsterdam: Elsevier. 2013. P. 765-788. DOI: 10.1016/B978-0-08-098258-8.00028-6.
20. **Rouquerol J., Llewellyn P., Rouquerol F.** Is the BET equation applicable to microporous adsorbents? *Stud. Surf. Sci. Catal.* 2007. V. 160. P. 49-56. DOI: 10.1016/S0167-2991(07)80008-5.
21. **Gil A., El Mouzdahir Y., Elmchaouri A., Vicente M.A., Korili S.A.** Equilibrium and thermodynamic investigation of methylene blue adsorption on thermal- and acid-activated clay minerals. *Desalin. Water Treat.* 2013. V. 51. Iss. 13-15. P. 2881-288. DOI: 10.1080/19443994.2012.748127.
22. **Pires J., Bestilleiro M., Pinto M., Gil A.** Selective adsorption of carbon dioxide, methane and ethane by porous clays heterostructures. *Separat. Purificat. Technol.* 2008. V. 61. N 2. P. 161-167. DOI: 10.1016/j.seppur.2007.10.007.
23. **Garces S.I., Villarroel-Rocha J., Sapag K., Korili S.A., Gil A.** Comparative Study of the Adsorption Equilibrium of CO_2 on Microporous Commercial Materials at Low Pressures. *Ind. Eng. Chem. Res.* 2013. V. 52. N 20. P. 6785-6793. DOI: 10.1021/ie400380w.
24. **Gil A., Trujillano R., Vicente M.A., Korili S.A.** Structure Evolution of Co/Alumina-Pillared Clay Catalysts under Thermal Treatment at Increasing Temperatures. *Ind. Eng. Chem. Res.* 2008. V. 47. N 19. P. 7226-7235. DOI: 10.1021/ ie071320v.
25. **Molu Z.B., Yurdakoc K.** Preparation and characterization of aluminum pillared K10 and KSF for adsorption of trimethoprim. *Micropor. Mesopor. Mater.* 2010. V. 127. N 1-2. P. 50-60. DOI: 10.1016/j.micromeso.2009.06.027.
26. **Xiao Y., He G., Yuan M.** Adsorption Equilibrium and Kinetics of Methanol Vapor on Zeolites NaX, KA, and CaA and Activated Alumina. *Ind. Eng. Chem. Res.* 2018. V. 57. N 42. P. 14254-14260. DOI: 10.1021/acs.iecr.8b04076.
27. **Centeno T.A., Stoeckli F.** The assessment of surface areas in porous carbons by two model-independent techniques, the DR equation and DFT. *Carbon*. 2010. V. 48. N 9. P. 2478-2486. DOI: 10.1016/j.carbon.2010.03.020.
28. **Sing K.S.W., Williams R.T.** Physisorption Hysteresis Loops and the Characterization of Nanoporous Materials. *Ads. Sci.Technol.* 2004. V. 22. N 10. P. 773-782. DOI: 10.1260/0263617053499032.
29. **Lecloux A., Pirard J.P.** The importance of standard isotherms in the analysis of adsorption isotherms for determining the porous texture of solids. *J. Colloid Interface Sci.* 1979. V. 70. Iss. 2. P. 265-281. DOI: 10.1016/0021-9797(79)90031-6.
30. **Brantley S.L., Mellott N.P.** Surface area and porosity of primary silicate minerals. *Am. Mineralogist.* 2000. V. 85. N 11-12. P. 1767-1783. DOI: 10.2138/am-2000-11-1220.
31. **Broekhoff J.C.P., de Boer J.H.** Surface Area Determination. 1969. London: Butterworths. P. 97–119. DOI: 10.1016/B978-0-408-70077-1.50013-0.
32. **Galarneau A., Ville F., Rodriguez J., Fajula F., Coasne B.** Validity of the t-plot Method to Assess Microporosity in Hierarchical Micro/Mesoporous Materials. *Langmuir*. 2014. V. 30. N 44. P. 13266-13274. DOI: 10.1021/la5026679.
33. **Polyakov N.S., Petukhova G.A.** Extension of the theory of volume filling of micropores to adsorption in supermicropores. *Adsorption*. 2005. V. 11. P. 357-362. DOI: 10.1007/s10450-005-5424-7.

Поступила в редакцию 20.10.2023
Принята к опубликованию 13.11.2023

Received 20.10.2023
Accepted 13.11.2023